CFD VALIDATION STUDY:

KCS_Case_2.1 - CALM WATER

NepTech

Intelligent sea mobility

Version	Date	Written by	Validated by
1	28/10/2024	Tanguy TEULET	Clément ROUSSET

Table of contents

Summary ***2***

Nomenclature ***3***

Figures ***3***

Tables ***3***

1. Tokyo 2015 Workshop on CFD Ship Hydrodynamics **4**

2. KRISO Container Ship **5**

3. Simulation setup **6**

a. Sign convention 6
b. Software's 6
c. Hypothesis 7
d. Numerical models 7
e. Validation 8

4. Results **11**

a. Comparison between the CFD and EFD model 11
b. Resistance 12
c. Resistance coefficient 13
d. Motions 14
e. Free surface renderings 16
f. Computational time comparison 18

5. Conclusion **19**

Bibliography ***20***

Summary

This report provides a comprehensive validation study on the KRISO Container Ship in calm water, conducted as part of the Tokyo 2015 Workshop on CFD Ship Hydrodynamics, using NepTech's digital towing tank. Key findings compare CFD results with experimental data, addressing resistance, resistance coefficients, vessel motions, free surface renderings, and computational time. Additionally, a mesh convergence study demonstrates the solution's stability and the exponential relationship between computation time and mesh count. The conclusion confirms the reliability and efficiency of NepTech's automated digital towing tank for low-Froude number monohull vessel simulations.

Nomenclature

- B_{WL} [m], waterline beam.
- C_B [−], block coefficient.
- EFD, Experimental fluid dynamic.
- $\mathrm{F_n}$ [−], Froude number.
- LCB [m], longitudinal centre of buoyancy.
- LCG ; TCG ; VCG [m], coordinates of the centre of gravity: lateral; transversal and vertical.
- $\mathrm{L_{WL}}$ [m], waterline length.
- S_w [m^2], wetted surface.
- T [m], draught.
- V [m/s], ship speed.
- ∇ [m^3], displacement.
- μ [Pa. s], dynamic viscosity.
- ρ [$\mathrm{kg/m}^3$], density.

Figures

Figure 1: Korean Container Ship (KCS) CAD model 5
Figure 2: Sign convention illustration 6
Figure 3: Free surface mesh for the different precision levels at 2.379 m/s = 4.625 knots 8
Figure 4: Bare hull mesh for the different precision levels at 2.379 m/s = 4.625 knots 9
Figure 5: Evolution (up), difference [N] (middle) and difference [%] (bottom) of total resistance 12
Figure 6: Evolution (up), difference [-] (middle) and difference [%] (bottom) of total resistance coefficient 13
Figure 7: Evolution (up), difference [m] (middle) and difference [%] (bottom) of dynamic heave attitude 14
Figure 8: Evolution (up), difference [deg] (middle) and difference [%] (bottom) of dynamic pitch attitude 15
Figure 9: Free surface evolution (same scale) 16
Figure 10: Free surface evolution (independent scale) 17
Figure 11: Computational time in hours 18

Tables

Table 1: Averaged number of cells 9
Table 2: Averaged Courant number 10
Table 3: Averaged Y+ 10
Table 4: Comparison between the CFD and EFD model 11

1. Tokyo 2015 Workshop on CFD Ship Hydrodynamics

The **Tokyo 2015 Workshop on CFD in Ship Hydrodynamics** was a pivotal event in the field of naval hydrodynamics, bringing together international experts to benchmark and assess state-of-the-art computational fluid dynamics (CFD) methods applied to ship flow problems. Building on a longstanding tradition of workshops on numerical methods in ship viscous flow, it continued the series that alternates between Gothenburg and Tokyo, following events held in Gothenburg in 1980, 1990, 2000, and 2010, and in Tokyo in 1994 and 2005. The 2015 workshop was held in Tokyo.

Organized by leading institutions, including the National Maritime Research Institute (Tokyo), Yokohama National University, Chalmers University of Technology (Sweden), IIHR (Iowa, USA), ECN (France), and KRISO (Korea), the event's objective was to evaluate the predictive capabilities of current numerical methods through a series of controlled test cases.

These test cases included three specific hull forms:

- The **Japan Bulk Carrier (JBC)**
- The **Korea Container Ship (KCS)**
- The **ONR Tumblehome Ship (ONRT)**

Unlike traditional conferences, the Tokyo 2015 workshop focused on collaborative assessment rather than individual presentations. Results and methods were presented via posters, and comprehensive evaluations were made for each hull, fostering in-depth discussions on improving accuracy and effectiveness in CFD modelling. Proceedings from the workshop captured the collective findings and insights, guiding the future development of CFD methods in ship hydrodynamics.

For detailed information on the hull geometries, test cases, and final workshop results, please visit the official Tokyo 2015 Workshop page here.

2. KRISO Container Ship

The **KRISO Container Ship (KCS)** is a benchmark hull form extensively used in naval hydrodynamics research to study ship performance and flow physics around vessels. Designed by the **Korea Research Institute for Ships and Ocean Engineering (KRISO)**, this modern container ship model from the late 1990s features a distinctive bulbous bow and a geometry representative of a typical commercial vessel of that era. While no full-scale ship has been built based on the KCS hull, this standardized design serves as a crucial reference for generating both experimental and CFD validation data.

Testing on the KCS hull has included a range of experiments, organized chronologically to provide essential datasets for validating CFD models against observed physical behaviour:

- 1998: **Resistance experiments** in towing tanks conducted by KRISO, capturing detailed measurements of resistance, free-surface waves, and mean flow data. (Van, Kim, Yim, Kim, & Lee, 1998)
- 2001: **Additional flow measurements** around modern commercial ship models, expanding upon KRISO's initial towing tank data. (Kim, Van, & Kim, 2001)
- 2005: **Self-propulsion tests** performed at the Ship Research Institute (now NMRI) in Tokyo, with findings published in the Proceedings of the CFD Workshop in Tokyo. (Hino, 2005)
- 2008: **Pitch, heave, and added resistance data** obtained, detailing the KCS hull's behaviour in heaving and pitching under regular head waves. (Simonsen, Otzen, & Stern, 2008)
- 2014: **Resistance, sinkage, and trim data** reported by NMRI, providing further insights into the hydrodynamic performance of the KCS. (Zou & Larsson, 2010)

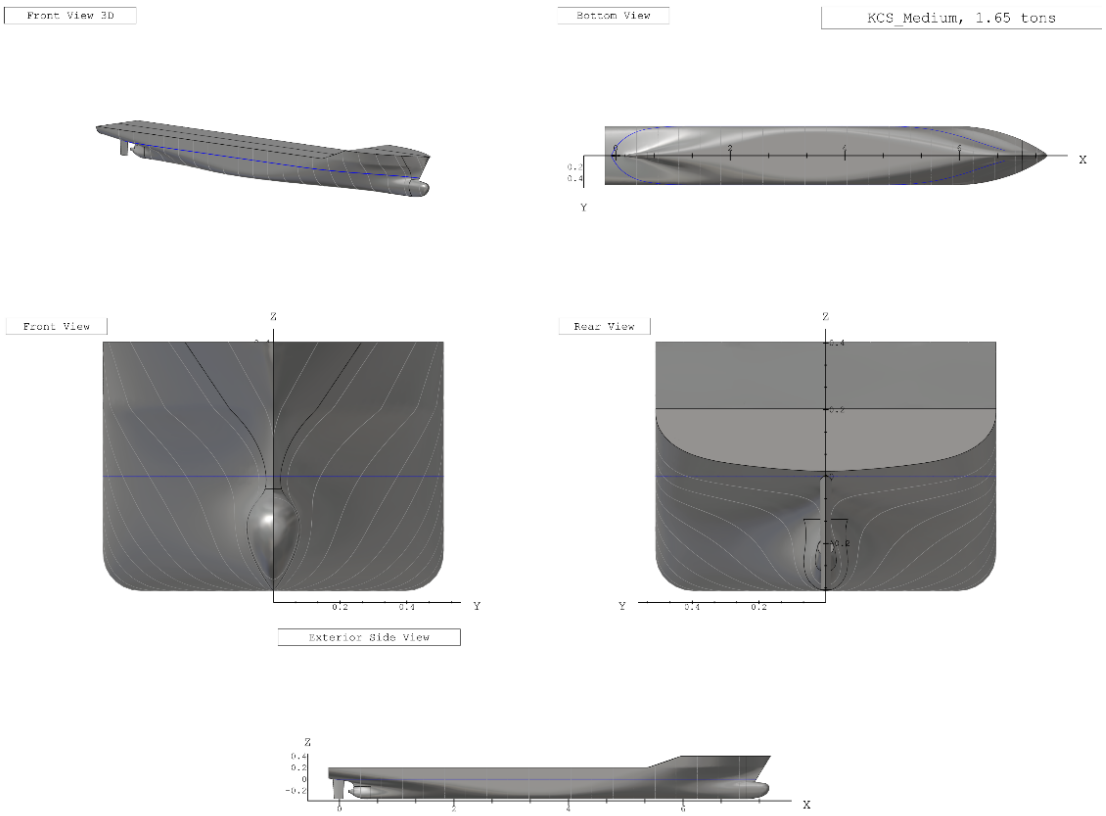

Figure 1: Korean Container Ship (KCS) CAD model

NepTech
Intelligent sea mobility

3. Simulation setup

a. Sign convention

Heave: The heave values correspond to the dynamic elevation of the vessel at the centre of gravity, relative to its hydrostatic position, in the absolute reference frame with the vertical axis Z oriented upwards. A positive heave value thus corresponds to a hull rise, while a negative value indicates the hull sinking.

Pitch: The pitch values correspond to the dynamic trim of the vessel at the centre of gravity, relative to its hydrostatic position, in the absolute reference frame where the transverse axis is Y. A positive trim corresponds to a bow-up attitude of the hull.

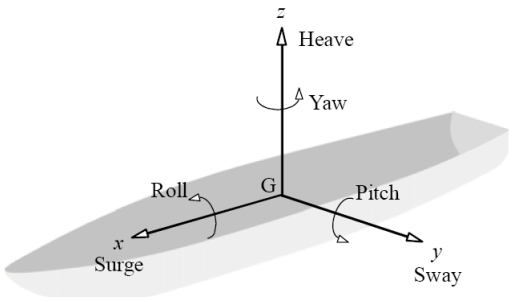

Figure 2: Sign convention illustration

b. Software's

Mesh: Hexpress™, version 12.1 developed by CADENCE

Resolution: Fidelity Fine Marine, version 12.1 developed by CADENCE

Solver: ISIS-CFD developed by CNRS and Centrale Nantes

Computing infrastructure: 2 virtual machines with 32 cores « STANDARD_F32S_V2 », optimized for computation on the Microsoft Azure cloud computing platform.

Post-processing:

- CFView™, version 12.1 developed by CADENCE
- Programming language Python version 3.11.6

c. Hypothesis

Modelling scale: model scale (1/31.6), with a symmetry plane along the vessel's median axis. This approach helps reduce computation time while maintaining identical results.

Domain: the dimensions of the simulation domain are conformed to International Towing Tank Conference (ITTC) recommendations, ensuring that the boundaries are positioned sufficiently far from the vessel to avoid any influence on the solution. It is crucial, especially for the exit boundary, to place it in a way that prevents the reflection of the wave field generated by the vessel.

Hydrostatic equilibrium: the coordinates of the centre of gravity are defined as follows

$$LCG = 3.53\,m;\ TCG = 0.00\,m;\ VCG = 0.01\,m$$

Water: corresponds to fresh water, which is

$$\rho_{water} = 995.5\ kg/m^3$$

$$\mu_{water} = 1.269 * 10^{-3}\ Pa.s$$

Air: corresponds to air at a temperature of $15°C$, which is

$$\rho_{air} = 1.2256\ kg/m^3$$

$$\mu_{air} = 1.788 * 10^{-5}\ Pa.s$$

Mesh precision: this report presents the results of a mesh convergence study conducted at four levels, referred to as coarse, medium, fine, and extra fine meshes. As the mesh precision level increases, both the surface refinement and the number of diffusion elements also rise. Moreover, as the mesh precision level increases, the pressure refinement criterion for the Adaptive Grid Refinement (AGR) decreases. This means that the AGR will increasingly refine the mesh in areas where a strong pressure gradient is observed within the flow. The fine and extra fine meshes are identical, except that the extra fine mesh has a volume refinement region at the Kelvin wedge.

d. Numerical models

Dynamic equilibrium:

- The Quasi-Static (QS) method is used since we are interested in the vessel's dynamic equilibrium state. This method relies on a succession of predictions of the vessel's physical attitude to reach the dynamic equilibrium state in record time.
- Two movements of the vessel, heave and pitch, are left free to ensure convergence toward the vessel's dynamic equilibrium position.

Flow: The Reynolds-Averaged Navier-Stokes (URANS) equations are used to describe the flow, and they are coupled with the $k - \omega\ SST$ turbulence model as the closure model.

Free surface: The air-water interface is modelled using the Volume of Fluid (VoF) method. Adaptive Grid Refinement (AGR), developed by CNRS (French National Centre for Scientific Research) and Ecole Centrale de Nantes (French Engineering school), is used to model the free surface. This iterative process allows for dynamic adjustment of the mesh according to the solution's needs during the calculation, making refinement decisions based on the physics of the flow.

e. Validation

i. Mesh

Free surface: The accuracy of the results regarding pressure resistance mainly depends on how the air-water interface is captured during simulation. This resistance is induced by the wave field generated by the vessel, and the quality of the mesh for the latter plays a crucial role in this accuracy. The use of AGR allows dynamically adapting the mesh based on the generated wave field, achieving maximum precision, as it is one of the most advanced and reliable methods to date and reducing computation time by converging more quickly toward the dynamic equilibrium state.

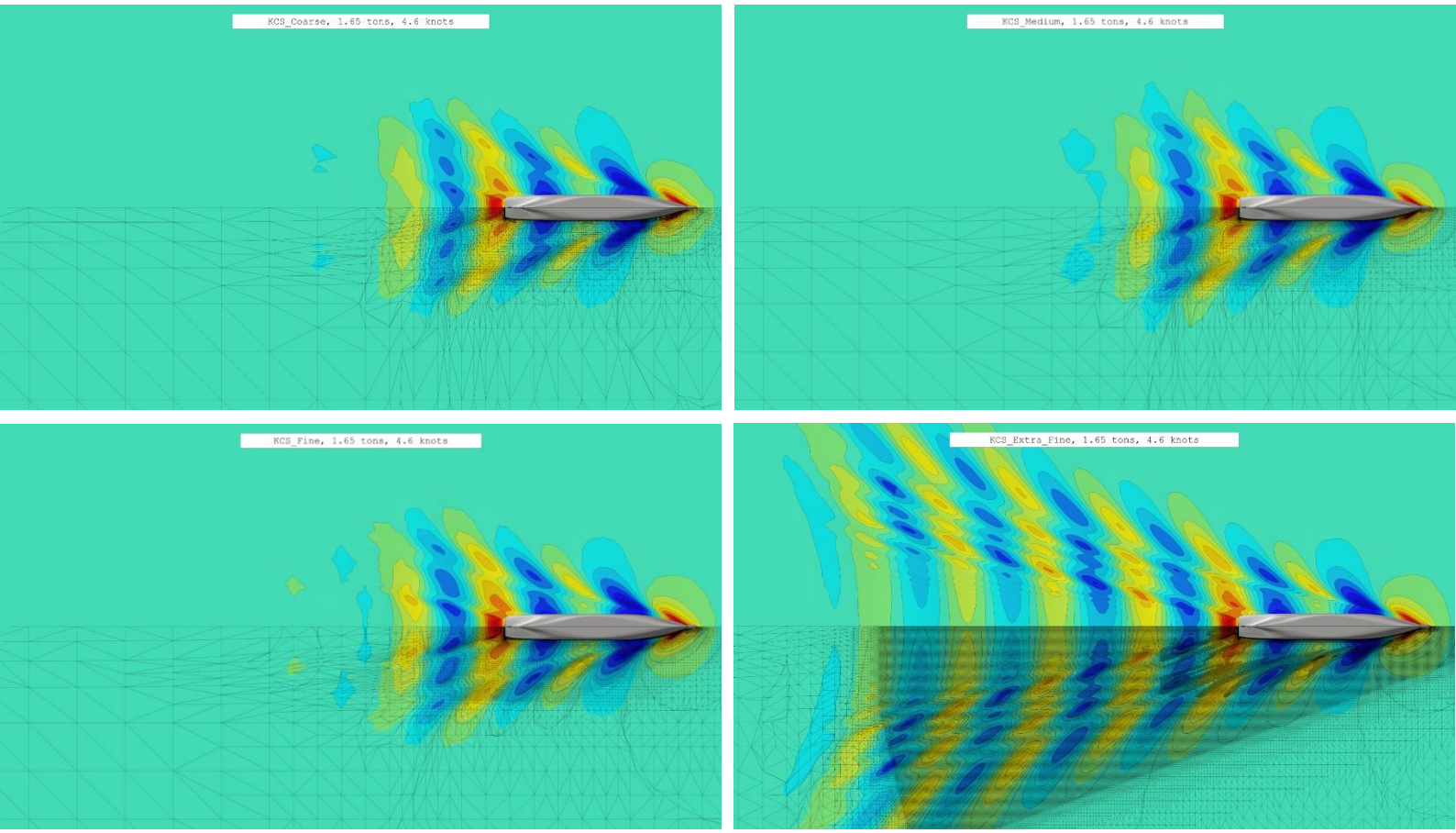

Figure 3: Free surface mesh for the different precision levels at 2.379 m/s = 4.625 knots

Hull: The accuracy of the results regarding viscous resistance mainly depends on the mesh of the hull. This resistance is caused by the entrainment of a thin fluid film: the boundary layer. An appropriate mesh of the boundary layer is essential to correctly capture local phenomena such as viscous effects and rapid variations in fluid properties near the surface. It also allows for better capture and resolution of turbulent phenomena if they are present. The quality of the hull mesh also affects the fidelity of the 3D model representation. A clean and regular mesh improves the reliability of the simulation, making the simulated model more representative of the actual vessel.

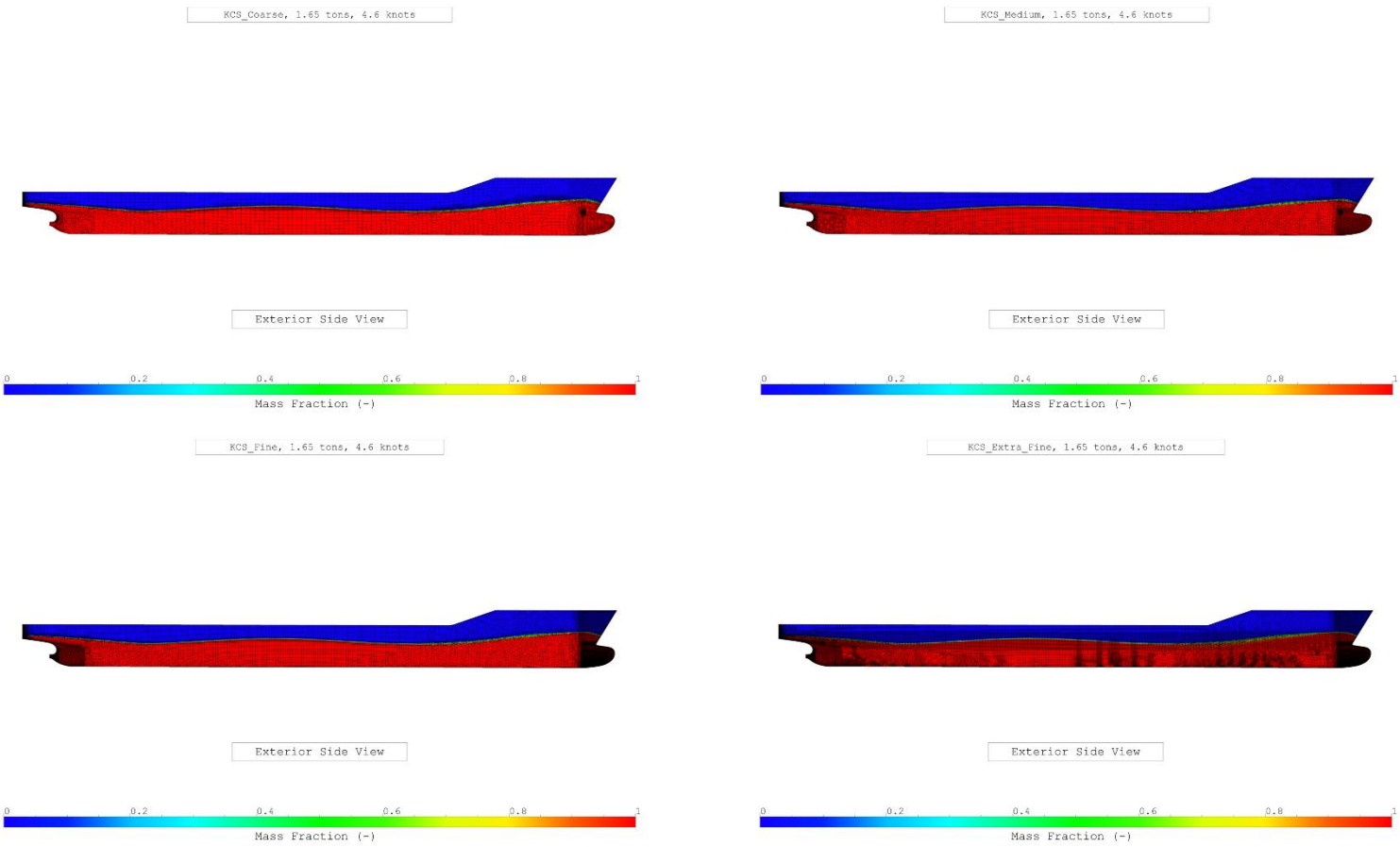

Figure 4: Bare hull mesh for the different precision levels at 2.379 m/s = 4.625 knots

Ship speed $\mathbf{V}$	$[\mathbf{m/s}]$	0.915	1.281	1.647	1.922	2.196	2.379
	$[\mathbf{knots}]$	1.779	2.490	3.202	3.736	4.269	4.625
Froude number $\mathbf{F_n}$ $[-]$		0.108	0.152	0.195	0.227	0.260	0.282
Averaged number of cells [*10^6]	Coarse mesh	0.37	0.39	0.39	0.39	0.40	0.41
	Medium mesh	0.70	0.73	0.74	0.74	0.75	0.76
	Fine mesh	1.30	1.37	1.36	1.35	1.36	1.37
	Extra fine mesh	3.60	4.33	5.31	6.26	7.68	8.86

Table 1: Averaged number of cells

ii. Courant number

Description: The Courant number, also called the CFL (Courant-Friedrichs-Lewy) number, is a crucial parameter in computational fluid dynamics (CFD). It measures the numerical stability of the discretization scheme used in the simulation. An inappropriate Courant number can lead to numerical instabilities, compromising both convergence and the accuracy of the results. In CFD, the Courant number is related to the size of the numerical time steps. It is calculated by comparing the speed of fluid particles with the size of the cells in the simulation domain.

Recommended values: For typical resistance simulations, it is recommended to keep the Courant number below or close to 1 to ensure maximum accuracy and reliability. Local spikes in this parameter may occur, but it is essential to control them to maintain numerical stability and the quality of the results.

Values:

Ship speed $\mathbf{V}$	$[\mathbf{m/s}]$	0.915	1.281	1.647	1.922	2.196	2.379
	$[\mathbf{knots}]$	1.779	2.490	3.202	3.736	4.269	4.625
Froude number $\mathbf{F_n}$ $[-]$		0.108	0.152	0.195	0.227	0.260	0.282
Averaged Courant number [-]	Coarse mesh	0.67	0.68	0.69	0.71	0.73	0.74
	Medium mesh	1.16	1.17	1.20	1.22	1.24	1.26
	Fine mesh	1.41	1.40	1.43	1.45	1.48	1.50
	Extra fine mesh	1.80	1.79	1.93	1.88	1.96	2.09

Table 2: Averaged Courant number

iii. Y+

Description: In the naval field, managing the Y+ parameter is crucial in computational fluid dynamics (CFD) simulations. Y+ measures the quality of the boundary layer resolution along the submerged surfaces of ship hulls by evaluating the distance between the first mesh point and the wall relative to the boundary layer thickness. Maintaining an appropriate Y+ is essential to ensure reliable results in predicting resistance, drag, lift, and other critical hydrodynamic phenomena. An improper Y+ can lead to significant errors in the prediction of forces, drag coefficients, and other key parameters.

Recommended values: For typical resistance simulations, it is recommended that the Y+ value be between 30 and 300. This value may be lower depending on the choice of boundary layer modeling. Local spikes in this parameter may occur, but it is essential to control them to maintain numerical stability and the quality of the results.

Values:

Ship speed $\mathbf{V}$	$[\mathbf{m/s}]$	0.915	1.281	1.647	1.922	2.196	2.379
	$[\mathbf{knots}]$	1.779	2.490	3.202	3.736	4.269	4.625
Froude number $\mathbf{F_n}$ $[-]$		0.108	0.152	0.195	0.227	0.260	0.282
Averaged Y+ [-]	Coarse mesh	35.80	41.90	52.73	60.80	68.67	73.97
	Medium mesh	37.17	43.62	55.02	63.45	71.65	77.26
	Fine mesh	37.67	43.61	55.02	63.46	71.69	77.25
	Extra fine mesh	37.09	36.95	37.58	37.96	38.16	38.47

Table 3: Averaged Y+

4. Results

a. Comparison between the CFD and EFD model

Comparing the hydrostatic data between a CFD model and an experimental model is crucial, though it's challenging due to the limitations of experimental CAD models, which are often numerically imperfect. These CAD files typically have surface irregularities or inconsistencies that can affect the accuracy of hydrostatic properties like displacement, block coefficient, and waterline length. Such discrepancies in hydrostatics can lead to differences in flow behaviour and resistance predictions between the CFD and experimental results.

Table 4 summarizes these differences, revealing that, despite a close approximation to the experimental model, notable discrepancies appear in wetted surface area, longitudinal centre of buoyancy, and block coefficient. These differences highlight the challenge of achieving perfect alignment between CFD and experimental models, as even minor variations in these hydrostatic parameters can significantly impact resistance and flow behaviour.

The variation in wetted surface area affects the frictional resistance component, while discrepancies in the longitudinal centre of buoyancy and block coefficient alter the hull's stability and pressure distribution along its length. These factors, though small individually, contribute cumulatively to differences in CFD and EFD results

Main particulars		EFD	CFD	Difference [%]
Length of waterline	L_{WL} $[m]$	7.358	7.391	0.45
Maximum beam of waterline	B_{WL} $[m]$	1.019	1.020	0.10
Draft	T $[m]$	0.342	0.342	0.00
Displacement volume	∇ $[m^3]$	1.649	1.645	-0.24
Wetted surface	S_w $[m^2]$	9.553	9.680	1.33
Longitudinal buoyancy centre	LCB $[m]$	3.494	3.529	1.00
Block coefficient	C_B $[-]$	0.650	0.640	-1.54

Table 4: Comparison between the CFD and EFD model

b. Resistance

Figure 5 illustrates the progression of the KCS resistance across different advance speeds in the top graph and table. The middle table shows the absolute differences between CFD and EFD in international units, while the bottom table displays the relative difference between CFD and EFD as a percentage:

$$E\%\ CFD = \frac{CFD - EFD}{EFD} * 100$$

To thoroughly assess results, particularly percentage differences, it is important to consider both percentage and absolute values. In comparisons with towing tank tests, target resistance values are very low, so even minor discrepancies can lead to large percentage errors.

The resistance error ranges from -1.66 to -0.07 Newtons (extra fine mesh), corresponding to -1.80 to -0.16 percent. This difference indicates that CFD underestimates resistance, which is expected since the CFD displacement and block coefficient are lower than those in the EFD, and the CFD waterline length is longer than in the EFD.

Mesh convergence is achieved with resistance values that closely approach EFD, although they remain slightly different due to minor variations in hull hydrostatics. Convergence is evident, as the difference in resistance between coarse and medium mesh sizes is larger than that between medium and fine, and finer to extra-fine meshes reduce the difference further.

	Speed [knots]	Froude number [-]	● KCS_Coarse	■ KCS_Medium	▲ KCS_Fine	★ KCS_Extra_Fine	+ KCS_EFD
0	1.78	0.11	16.65	15.48	15.27	15.07	15.21
1	2.49	0.15	29.89	28.69	28.37	28.23	28.51
2	3.20	0.19	46.80	45.41	45.01	44.81	44.88
3	3.74	0.23	63.49	61.58	61.07	60.93	61.31
4	4.27	0.26	88.18	85.31	84.07	83.90	85.44
5	4.62	0.28	123.38	121.48	120.32	119.66	121.32

	Speed [knots]	Froude number [-]	X_0 = KCS_Coarse, [N]	X_1 = KCS_Medium, [N]	X_2 = KCS_Fine, [N]	X_3 = KCS_Extra_Fine, [N]
0	1.78	0.11	1.44	0.27	0.06	-0.14
1	2.49	0.15	1.38	0.18	-0.14	-0.28
2	3.20	0.19	1.92	0.53	0.13	-0.07
3	3.74	0.23	2.18	0.27	-0.24	-0.38
4	4.27	0.26	2.74	-0.13	-1.37	-1.54
5	4.62	0.28	2.06	0.16	-1.00	-1.66

	Speed [knots]	Froude number [-]	X_0 = KCS_Coarse, [%]	X_1 = KCS_Medium, [%]	X_2 = KCS_Fine, [%]	X_3 = KCS_Extra_Fine, [%]
0	1.78	0.11	9.47	1.78	0.39	-0.92
1	2.49	0.15	4.84	0.63	-0.49	-0.98
2	3.20	0.19	4.28	1.18	0.29	-0.16
3	3.74	0.23	3.56	0.44	-0.39	-0.62
4	4.27	0.26	3.21	-0.15	-1.60	-1.80
5	4.62	0.28	1.70	0.13	-0.82	-1.37

Figure 5: Evolution (up), difference [N] (middle) and difference [%] (bottom) of total resistance

c. Resistance coefficient

Figure 6 illustrates the progression of the KCS resistance coefficient across different advance speeds in the top graph and table. The middle table shows the absolute differences between CFD and EFD in international units, while the bottom table displays the relative difference between CFD and EFD as a percentage.

The resistance coefficient error between EFD and CFD ranges from $7.00e^{-5}$ to $-1.10e^{-4}$, corresponding to -1.15 to -2.70 percent.

The same conclusions apply here as for the resistance values.

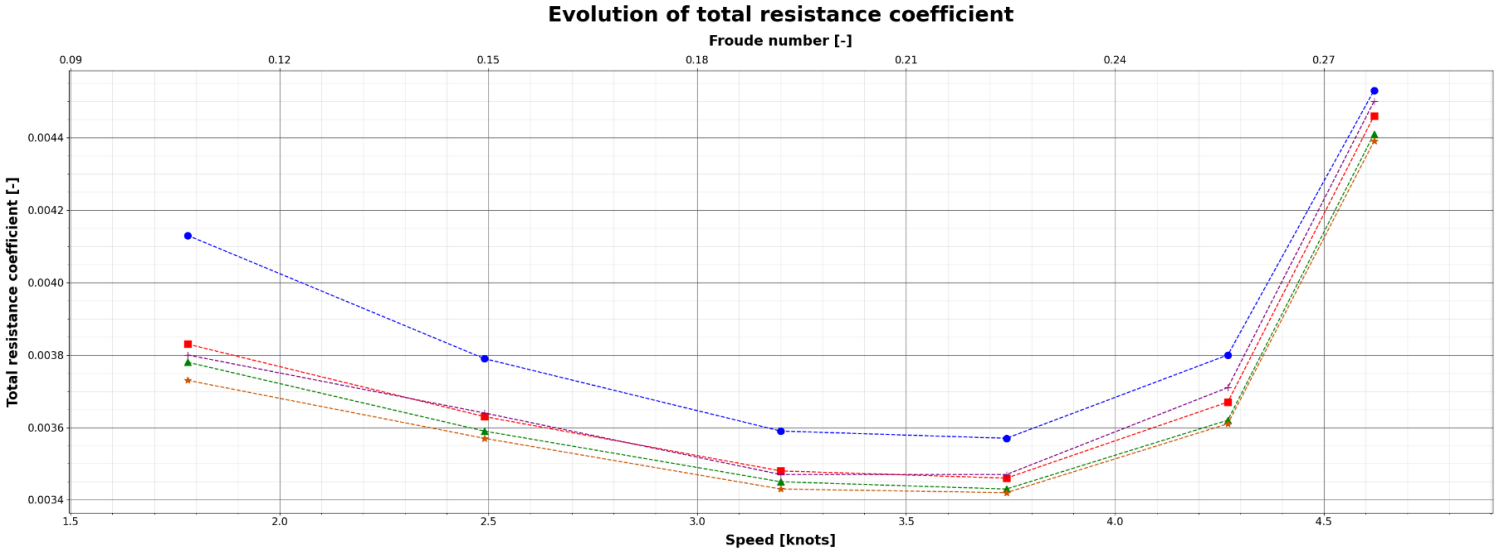

	Speed [knots]	Froude number [-]	● KCS_Coarse	■ KCS_Medium	▲ KCS_Fine	★ KCS_Extra_Fine	+ KCS_EFD
0	1.78	0.11	4.13e-03	3.83e-03	3.78e-03	3.73e-03	3.80e-03
1	2.49	0.15	3.79e-03	3.63e-03	3.59e-03	3.57e-03	3.64e-03
2	3.20	0.19	3.59e-03	3.48e-03	3.45e-03	3.43e-03	3.47e-03
3	3.74	0.23	3.57e-03	3.46e-03	3.43e-03	3.42e-03	3.47e-03
4	4.27	0.26	3.80e-03	3.67e-03	3.62e-03	3.61e-03	3.71e-03
5	4.62	0.28	4.53e-03	4.46e-03	4.41e-03	4.39e-03	4.50e-03

	Speed [knots]	Froude number [-]	X_0 = KCS_Coarse, [-]	X_1 = KCS_Medium, [-]	X_2 = KCS_Fine, [-]	X_3 = KCS_Extra_Fine, [-]
0	1.78	0.11	3.30e-04	3.00e-05	-2.00e-05	-7.00e-05
1	2.49	0.15	1.50e-04	-1.00e-05	-5.00e-05	-7.00e-05
2	3.20	0.19	1.20e-04	1.00e-05	-2.00e-05	-4.00e-05
3	3.74	0.23	1.00e-04	-1.00e-05	-4.00e-05	-5.00e-05
4	4.27	0.26	9.00e-05	-4.00e-05	-9.00e-05	-1.00e-04
5	4.62	0.28	3.00e-05	-4.00e-05	-9.00e-05	-1.10e-04

	Speed [knots]	Froude number [-]	X_0 = KCS_Coarse, [%]	X_1 = KCS_Medium, [%]	X_2 = KCS_Fine, [%]	X_3 = KCS_Extra_Fine, [%]
0	1.78	0.11	8.68	0.79	-0.53	-1.84
1	2.49	0.15	4.12	-0.27	-1.37	-1.92
2	3.20	0.19	3.46	0.29	-0.58	-1.15
3	3.74	0.23	2.88	-0.29	-1.15	-1.44
4	4.27	0.26	2.43	-1.08	-2.43	-2.70
5	4.62	0.28	0.67	-0.89	-2.00	-2.44

Figure 6: Evolution (up), difference [-] (middle) and difference [%] (bottom) of total resistance coefficient

d. Motions

For motion analysis, it is essential to keep in mind the existing differences between the CFD model and the experimental model, particularly the variation in the longitudinal centre of buoyancy and the wetted surface area, which has a significant impact on the hull's motion response.

i. Heave

Figure 7 illustrates the progression of the KCS dynamic heave response across different advance speeds in the top graph and table. The middle table shows the absolute differences between CFD and EFD in international units, while the bottom table displays the relative difference between CFD and EFD as a percentage.

To thoroughly assess results, particularly percentage differences, it is important to consider both percentage and absolute values. In comparisons with towing tank tests, target dynamic heave values are very low, so even minor discrepancies can lead to large percentage errors.

The dynamic heave error between EFD and CFD is on the order of millimetres.

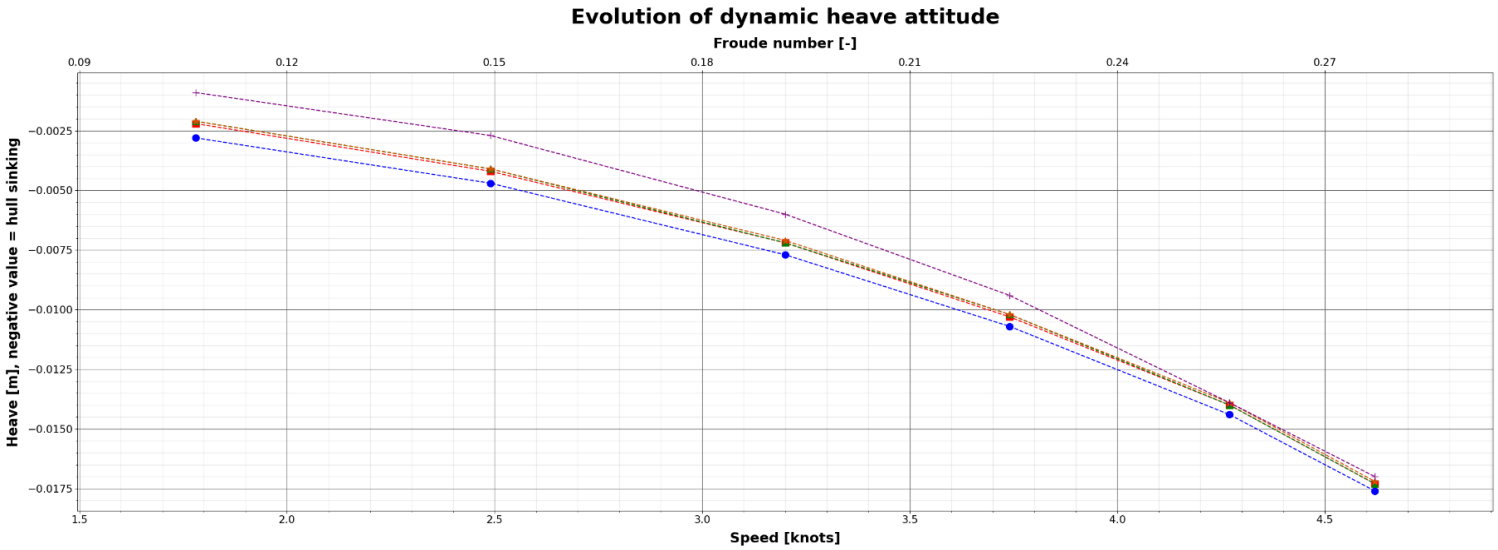

	Speed [knots]	Froude number [-]	● KCS_Coarse	■ KCS_Medium	▲ KCS_Fine	★ KCS_Extra_Fine	+ KCS_EFD
0	1.78	0.11	-0.0028	-0.0022	-0.0021	-0.0021	-0.0009
1	2.49	0.15	-0.0047	-0.0042	-0.0041	-0.0041	-0.0027
2	3.20	0.19	-0.0077	-0.0072	-0.0072	-0.0071	-0.0060
3	3.74	0.23	-0.0107	-0.0103	-0.0102	-0.0102	-0.0094
4	4.27	0.26	-0.0144	-0.0140	-0.0140	-0.0139	-0.0139
5	4.62	0.28	-0.0176	-0.0173	-0.0173	-0.0172	-0.0170

	Speed [knots]	Froude number [-]	X_0 = KCS_Coarse, [m]	X_1 = KCS_Medium, [m]	X_2 = KCS_Fine, [m]	X_3 = KCS_Extra_Fine, [m]
0	1.78	0.11	-0.002	-0.001	-0.001	-0.001
1	2.49	0.15	-0.002	-0.001	-0.001	-0.001
2	3.20	0.19	-0.002	-0.001	-0.001	-0.001
3	3.74	0.23	-0.001	-0.001	-0.001	-0.001
4	4.27	0.26	-0.001	-0.000	-0.000	0.000
5	4.62	0.28	-0.001	-0.000	-0.000	-0.000

	Speed [knots]	Froude number [-]	X_0 = KCS_Coarse, [%]	X_1 = KCS_Medium, [%]	X_2 = KCS_Fine, [%]	X_3 = KCS_Extra_Fine, [%]
0	1.78	0.11	211.11	144.44	133.33	133.33
1	2.49	0.15	74.07	55.56	51.85	51.85
2	3.20	0.19	28.33	20.00	20.00	18.33
3	3.74	0.23	13.83	9.57	8.51	8.51
4	4.27	0.26	3.60	0.72	0.72	-0.00
5	4.62	0.28	3.53	1.76	1.76	1.18

Figure 7: Evolution (up), difference [m] (middle) and difference [%] (bottom) of dynamic heave attitude

ii. Pitch

Figure 8 illustrates the progression of the KCS dynamic pitch response across different advance speeds in the top graph and table. The middle table shows the absolute differences between CFD and EFD in degrees, while the bottom table displays the relative difference between CFD and EFD as a percentage.

To thoroughly assess results, particularly percentage differences, it is important to consider both percentage and absolute values. In comparisons with towing tank tests, target dynamic pitch values are very low, so even minor discrepancies can lead to large percentage errors.

The dynamic pitch error between EFD and CFD ranges from -0.003 to -0.012 degrees, corresponding to plus or minus 16 percent.

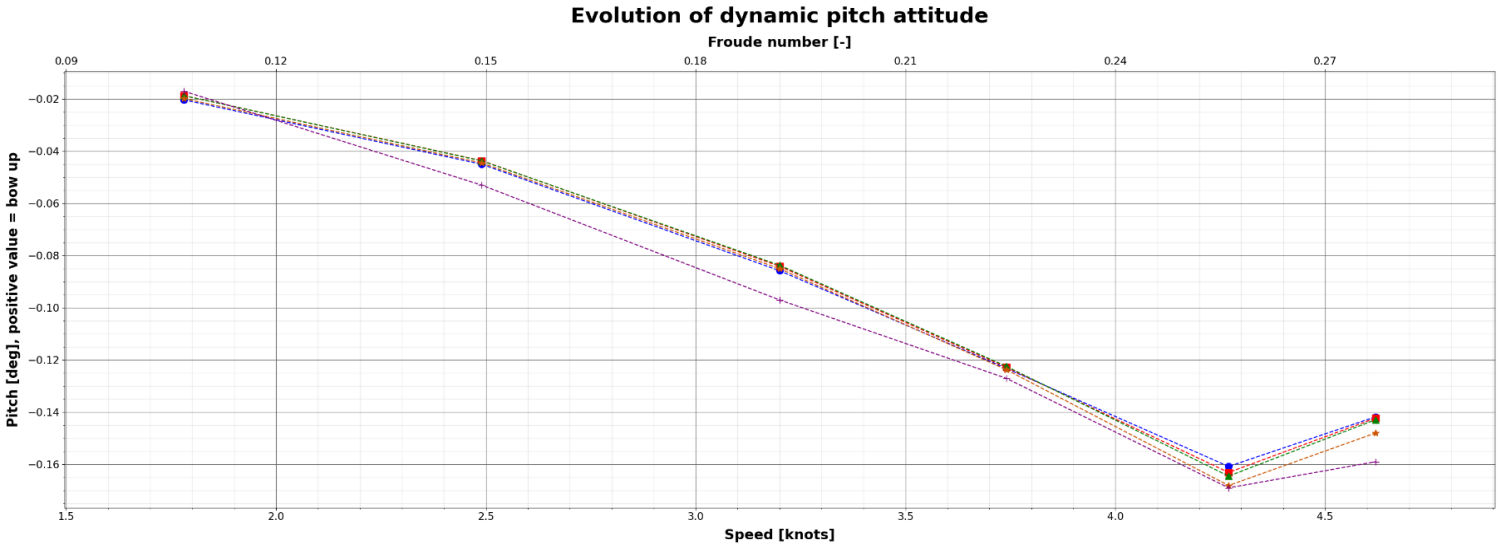

	Speed [knots]	Froude number [-]	● KCS_Coarse	■ KCS_Medium	▲ KCS_Fine	★ KCS_Extra_Fine	+ KCS_EFD
0	1.78	0.11	-0.0203	-0.0187	-0.0187	-0.0198	-0.0170
1	2.49	0.15	-0.0450	-0.0436	-0.0437	-0.0445	-0.0530
2	3.20	0.19	-0.0858	-0.0841	-0.0837	-0.0850	-0.0970
3	3.74	0.23	-0.1232	-0.1228	-0.1224	-0.1237	-0.1270
4	4.27	0.26	-0.1608	-0.1631	-0.1645	-0.1681	-0.1690
5	4.62	0.28	-0.1418	-0.1423	-0.1429	-0.1480	-0.1590

	Speed [knots]	Froude number [-]	X_0 = KCS_Coarse, [deg]	X_1 = KCS_Medium, [deg]	X_2 = KCS_Fine, [deg]	X_3 = KCS_Extra_Fine, [deg]
0	1.78	0.11	-0.003	-0.002	-0.002	-0.003
1	2.49	0.15	0.008	0.009	0.009	0.009
2	3.20	0.19	0.011	0.013	0.013	0.012
3	3.74	0.23	0.004	0.004	0.005	0.003
4	4.27	0.26	0.008	0.006	0.005	0.001
5	4.62	0.28	0.017	0.017	0.016	0.011

	Speed [knots]	Froude number [-]	X_0 = KCS_Coarse, [%]	X_1 = KCS_Medium, [%]	X_2 = KCS_Fine, [%]	X_3 = KCS_Extra_Fine, [%]
0	1.78	0.11	19.41	10.00	10.00	16.47
1	2.49	0.15	-15.09	-17.74	-17.55	-16.04
2	3.20	0.19	-11.55	-13.30	-13.71	-12.37
3	3.74	0.23	-2.99	-3.31	-3.62	-2.60
4	4.27	0.26	-4.85	-3.49	-2.66	-0.53
5	4.62	0.28	-10.82	-10.50	-10.13	-6.92

Figure 8: Evolution (up), difference [deg] (middle) and difference [%] (bottom) of dynamic pitch attitude

e. Free surface renderings

i. Same scale

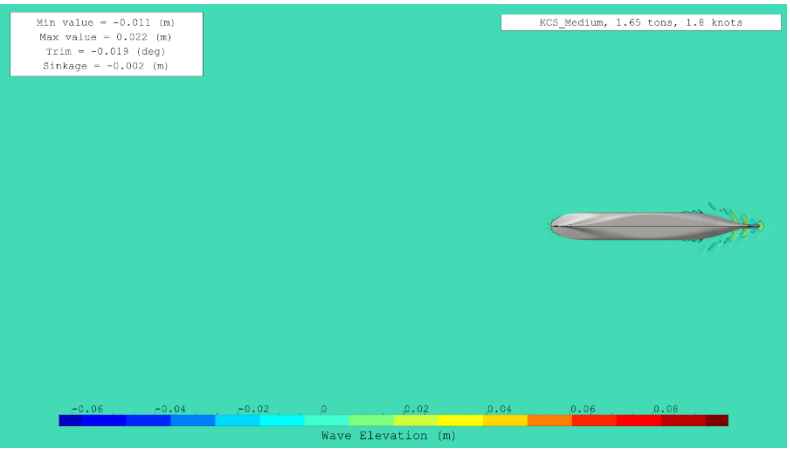

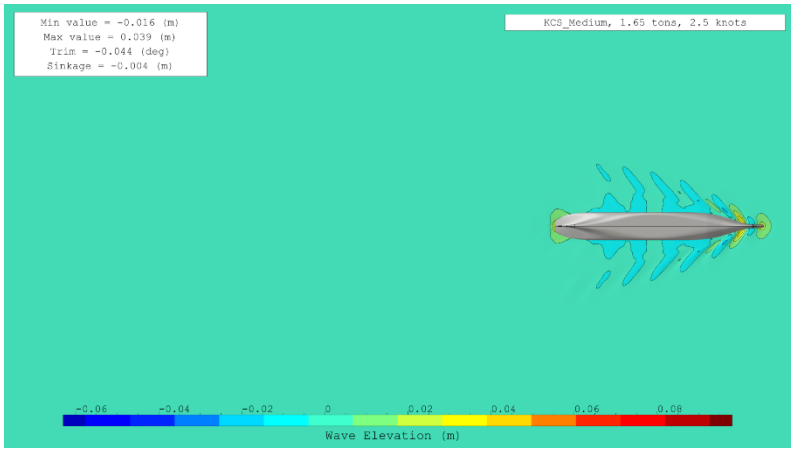

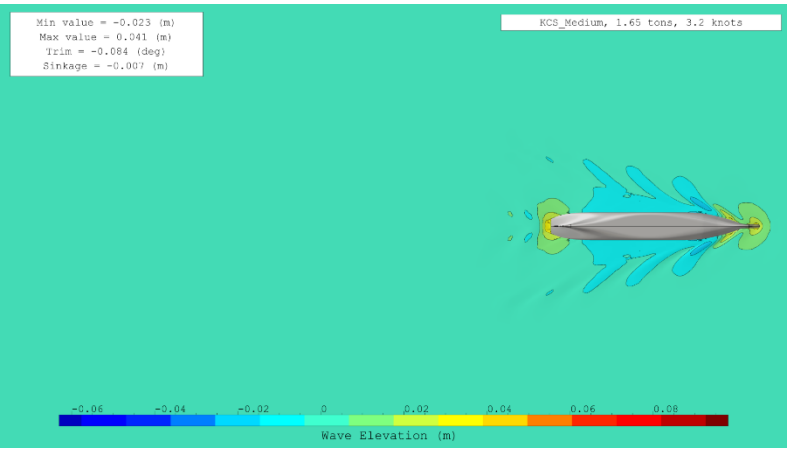

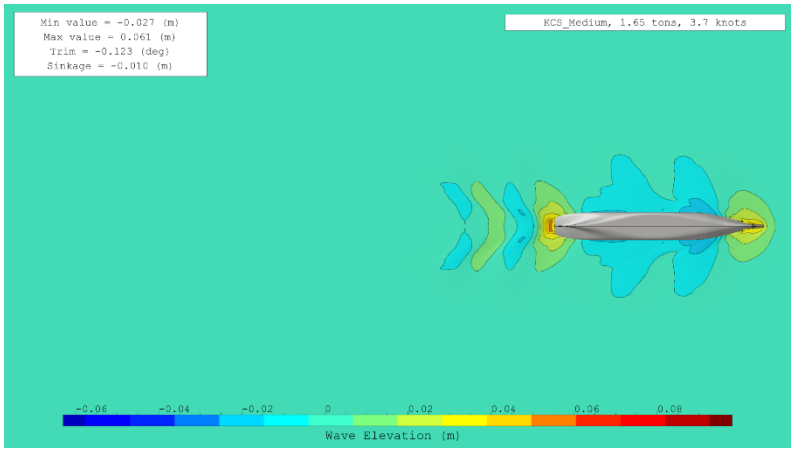

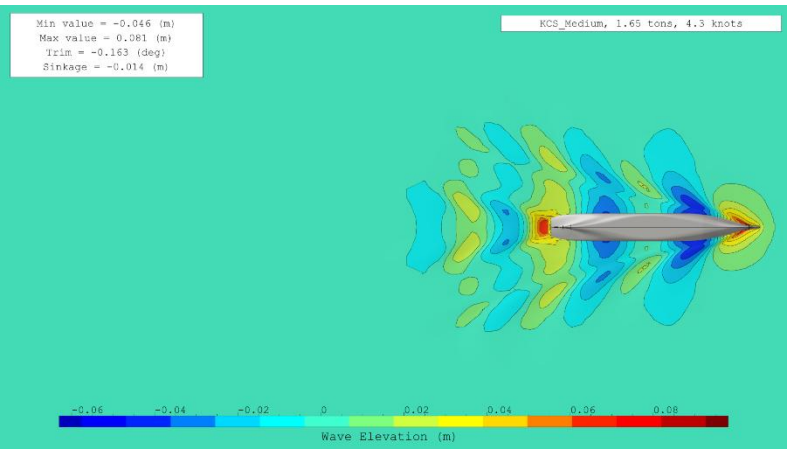

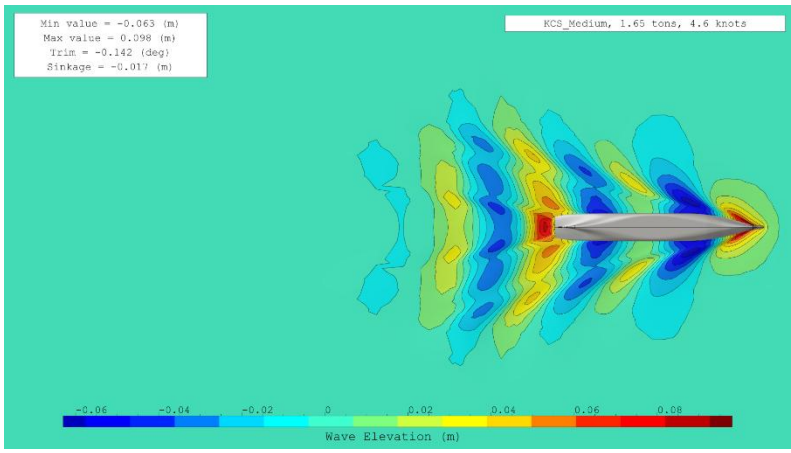

Figure 9: Free surface evolution (same scale)

ii. Independent scale

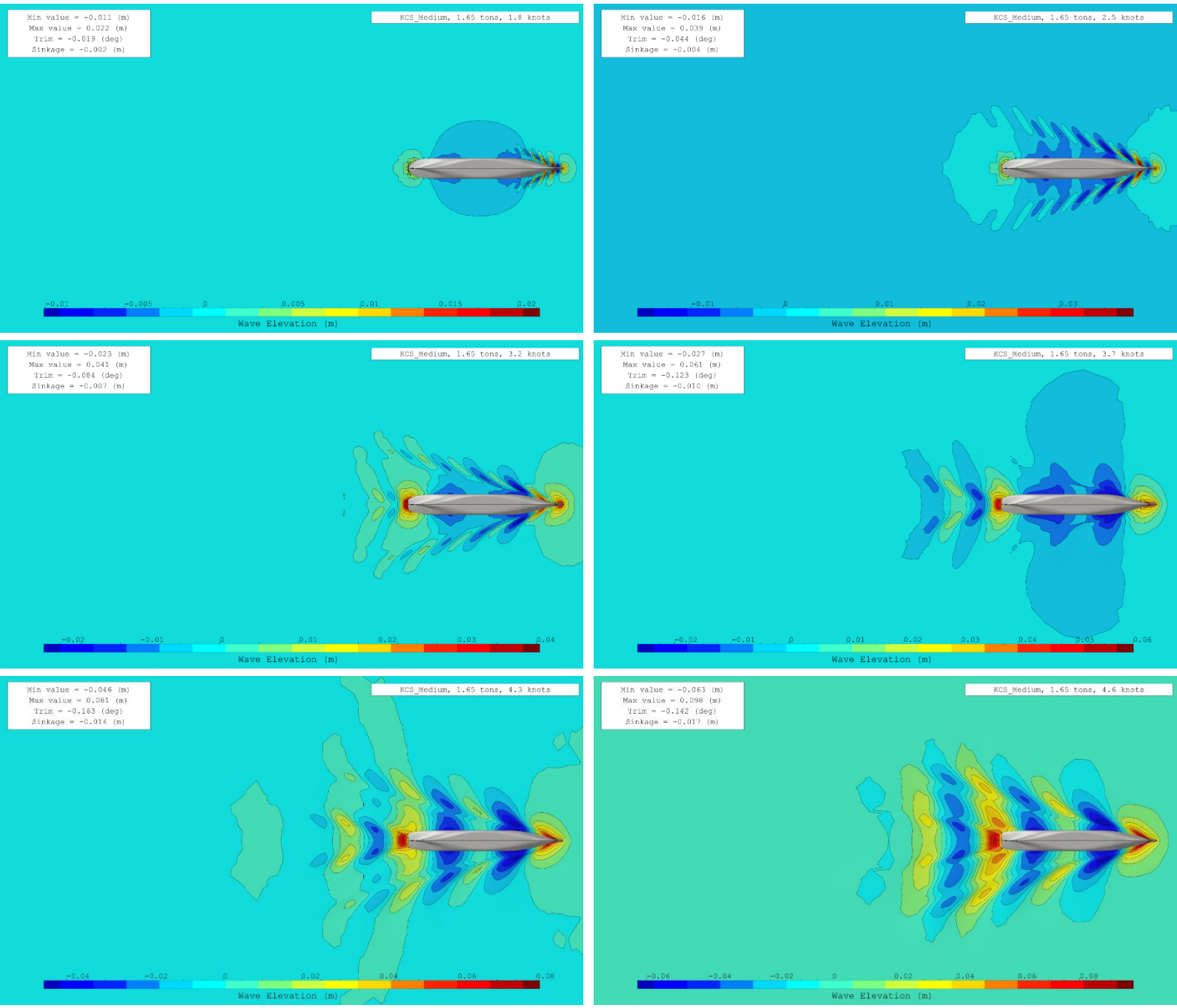

Figure 10: Free surface evolution (independent scale)

f. Computational time comparison

Figure 11 compares the computation times, in hours, across different mesh configurations. Since we run simulations on an optimal number of cores determined by the mesh cell count, it is crucial to consider the number of cores utilized.

It is also important to note that this optimal core count is not achieved for the extra-fine mesh due to a limitation imposed by the license, which is capped at 32 cores.

Notably, for a medium mesh that produces more than acceptable results, we complete the entire resistance curve calculation in approximately 9 hours, which is exceptionally efficient for performing six CFD simulations.

	Speed [knots]	Froude number [-]	● Core [-]	● KCS_Coarse	■ Core [-]	■ KCS_Medium	▲ Core [-]	▲ KCS_Fine	★ Core [-]	★ KCS_Extra_Fine
0	1.78	0.11	4	0.77	7	0.77	13	1.42	32	10.05
1	2.49	0.15	4	0.73	7	0.98	13	1.47	32	4.62
2	3.20	0.19	4	0.77	7	1.03	13	1.43	32	5.40
3	3.74	0.23	4	2.68	7	3.53	13	4.83	32	22.40
4	4.27	0.26	4	1.17	7	1.33	13	1.82	32	11.55
5	4.62	0.28	4	1.13	7	1.57	13	2.08	32	15.18

Figure 11: Computational time in hours

5. Conclusion

This report presents a validation study conducted to predict the calm-water resistance of the KRISO Container Ship, comparing results obtained using NepTech's digital towing tank with available experimental data from Korea Research Institute of Ships & Ocean Engineering (KRISO) and the National Maritime Research Institute (NMRI) from the Tokyo 2015 Workshop on CFD in Ship Hydrodynamics.

The findings demonstrate a strong correlation between the numerical and experimental results, with:

- A resistance error ranging from -1.66 to -0.07 Newtons*, equating to -1.80 to -0.16 percent,
- A heave error on the order of millimetres,
- A dynamic pitch error from -0.003 to -0.012 degrees*, corresponding to a variation of approximately ±16 percent.

*for the extra fine mesh

The EFD/CFD differences can be attributed to variations in hydrostatic characteristics between the model used for the tank tests and the model applied in CFD calculations.

A mesh convergence study further demonstrated convergence while highlighting the exponential increase in computational time as a function of mesh cell count.

This report thus confirms NepTech's capability to accurately and efficiently predict the dynamic behaviour of a monohull vessel advancing at low speeds. By employing a fully automated digital towing tank using the latest advanced modelling tools, we conclude that simulations of similar flow type will be reliable.

Bibliography

Hino, T. (2005). *Proceedings of CFD Workshop Tokyo 2005.* NMRI.

Kim, W., Van, D., & Kim, D. (2001). Measurement of flows around modern commercial ship models. *Experiments in Fluids, Volume 31*, 567-578.

Simonsen, C., Otzen, J., & Stern, F. (2008). EFD and CFD for KCS heaving and pitching in regular head waves. *Proceedings 27th Symposium on Naval Hydrodynamics.* Seoul, Korea.

Van, S., Kim, W., Yim, G., Kim, D., & Lee, C. (1998). Experimental Investigation of the Flow Characteristics Around Practical Hull Forms. *Proceedings 3rd Osaka Colloquium on Advanced CFD Applications to Ship Flow and Hull Form Design.* Osaka, Japan.

Zou, L., & Larsson, L. (2010). *Additional data for resistance, sinkage and trim.* Doordrecht: Larsson et al "Numerical Ship Hydrodynamics - An Assessment of the Gothenburg 2010 Workshop".